



Short communication

Development of a protocol to quantify local bone adaptation over space and time: Quantification of reproducibility

Yongtao Lu^{a,b,*}, Maya Boudiffa^c, Enrico Dall'Ara^c, Iliaria Bellantuono^c, Marco Viceconti^b^a Department of Engineering Mechanics, Dalian University of Technology, Dalian, China^b Department of Mechanical Engineering and INSIGNEO Institute for in Silico Medicine, the University of Sheffield, Sheffield, UK^c Department of Oncology and Metabolism and INSIGNEO Institute for in Silico Medicine, University of Sheffield, Sheffield, UK

ARTICLE INFO

Article history:

Accepted 18 May 2016

Keywords:

In vivo micro-CT
Local bone adaptation
Mouse tibia
Space and time

ABSTRACT

In vivo micro-computed tomography (μ CT) scanning of small rodents is a powerful method for longitudinal monitoring of bone adaptation. However, the life-time bone growth in small rodents makes it a challenge to quantify local bone adaptation. Therefore, the aim of this study was to develop a protocol, which can take into account large bone growth, to quantify local bone adaptations over space and time. The entire right tibiae of eight 14-week-old C57BL/6J female mice were consecutively scanned four times in an *in vivo* μ CT scanner using a nominal isotropic image voxel size of 10.4 μ m. The repeated scan image datasets were aligned to the corresponding baseline (first) scan image dataset using rigid registration. 80% of tibia length (starting from the endpoint of the proximal growth plate) was selected as the volume of interest and partitioned into 40 regions along the tibial long axis (10 divisions) and in the cross-section (4 sectors). The bone mineral content (BMC) was used to quantify bone adaptation and was calculated in each region. All local BMCs have precision errors ($PE_{\%CV}$) of less than 3.5% (24 out of 40 regions have $PE_{\%CV}$ of less than 2%), least significant changes (LSCs) of less than 3.8%, and 38 out of 40 regions have intraclass correlation coefficients (ICCs) of over 0.8. The proposed protocol allows to quantify local bone adaptations over an entire tibia in longitudinal studies, with a high reproducibility, an essential requirement to reduce the number of animals to achieve the necessary statistical power.

© 2016 The Authors. Published by Elsevier Ltd. This is an open access article under the CC BY-NC-ND license (<http://creativecommons.org/licenses/by-nc-nd/4.0/>).

1. Introduction

Bone adaptation is a process in which bone undergoes adaptive changes. While bone keeps its strength through balanced resorption and formation, disorder of bone adaptation can lead to bone diseases, such as osteoporosis, osteomalacia, Paget's disease, etc. (Britton and Walsh, 2012; Shih 2012). Small rodents offer a cost-effective and efficient way for the investigation of bone diseases in preclinical studies. In addition, the development of *in vivo* high resolution micro-computed tomography (μ CT) scanning on the entire bone of small rodents offers a powerful approach to quantify bone adaptations over space and time (Altman et al., 2015; Birkhold et al., 2014; Lambers et al., 2013; Lu et al., 2015). To quantify bone adaptations, three-dimensional (3D) bone morphometric measurements (trabecular thickness, trabecular separation, cortex thickness, etc.) over a volume of interest (VOI)

(proximal mouse tibia, tibial midshaft, etc.) were used (Bouxsein et al., 2010; Campbell et al., 2014; Lambers et al., 2013; Nishiyama et al., 2010). Although 3D image registration can improve the long-term precision of these measurements (Campbell et al., 2014), these morphometric measurements were averaged values over a region of an entire bone and can hardly be used to quantify local bone adaptations over the entire bone's space. On the contrary, *in vivo* μ CT images obtained at the same anatomical site over different time points were superimposed using the rigid registration, and then bone formation and resorption were quantified from the superimposed images (Birkhold et al., 2014; Schulte et al., 2011). However, in rodents like mouse, bone growth spans across the animal's life time (Glatt et al., 2007), and should be taken into account when interpreting the data (Birkhold et al., 2014). This is particular true for long bones (e.g. tibia), where changes in length due to growth can be significant. In this case, it may still be valid to quantify bone formation and resorption over a short time interval with rigidly registered images (Birkhold et al., 2014), but this approach would fail in a longer time interval (e.g. 2 weeks) due to the significant shift and changes of bone structure caused by bone growth. Therefore, in this study, a novel protocol that aims to

* Correspondence to: Department of Engineering Mechanics Dalian University of Technology, LingGong Road 2, GanJingzi District, 116024 Dalian, China.
Tel.: +86 (0) 411 84707029.

E-mail addresses: yongtaolu@dlut.edu.cn, yongtaolu@hotmail.com (Y. Lu).

account for large bone growth was proposed to quantify the local bone adaptation over a larger volume of interest (80% of mouse tibia) and over space and time.

2. Material and methods

2.1. Animals

The detailed information on animals can be found in Lu et al. (2015). In summary, eight 14-week-old female C57BL/6J (BL6) mice were used and the mice were well housed before the experiment. All the procedures were approved by the local Research Ethics Committee of the University of Sheffield (Sheffield, UK).

2.2. In vivo μ CT scanning

The details of the *in vivo* μ CT scanning were in Lu et al. (2015). In summary, the entire right tibia of every mouse was scanned four times consecutively (the scanning of each tibia took approximately 40 min) with an *in vivo* μ CT system (vivaCT 80, Scanco Medical, Bruettisellen, Switzerland) at 14-week-old. For the duration of the scanning, the mice were placed on a heating pad, maintained under anaesthetic gases (isoflurane). Between each scan, the mouse (kept under anaesthesia) was repositioned in the sample holder to simulate a longitudinal study design. The scanner was operated at 55 keV, 145 μ A, an integration time of 200 ms and a nominal isotropic image voxel size of 10.4 μ m. The radiation dose from the μ CT scanning was estimated to be approximately 500 mGy for each scan, which has been proved to cause no significant effect on bone adaptations (Laperre et al., 2011).

2.3. Image processing and calculation of bone parameters

In the image processing chain, first, an alignment procedure was defined so that all tibiae, regardless of their positions in the scanner, were aligned to the same anatomical reference system. In the alignment procedure, the tibia from the

baseline scan was taken as the reference, referred as baseline scan 1 thereafter. The tibia of the baseline scan 1 (Fig. 1a) was placed back into its anatomical position, i.e. the long axis of the tibia was approximately aligned with the global z axis and the y-z plane passed through the centre line of the articular surfaces of the medial and lateral condyles (Fig. 1b). The tibiae from the repeated scans and from other mice were rigidly registered and transformed to the transformed tibia of baseline scan 1 (Fig. 1d) and then resampled using the Lanczos kernel (Turkowski and Gabriel, 1990).

After the image transformation, the tibial length (L) was measured as the distance from the most proximal tibial bone pixel until the most distal tibial bone pixel. Afterwards, a region of 80% of L (Fig. 1d), starting from the end of the proximal growth plate (Klinck et al., 2008) was cropped out [Amira 5.4.3, FEI Visualization Sciences Group, France]. Then the tibial VOI was extracted by removing the proximal part of fibula (Fig. 1e and f) (Matlab v2015a, the Mathworks, Inc. USA).

To investigate the spatial adaptation of the Bone Mineral Content (BMC), the tibial VOI was partitioned into 40 sub-volumes. In the tibial longitudinal (proximal-distal) direction, the tibial VOI was divided into 10 regions (Fig. 1e). In the tibial transverse (x-y) section, a polar coordinate system was created for each image slice. The system was originated at the centre of mass of each slice and the x-axis was defined from the tibial medial side towards the lateral side (Fig. 1g). In the tibial transverse section, the tibia was then divided into 4 sectors (anterior, medial, posterior and lateral sectors), starting from the position that is 45° away from the x-axis (Fig. 1g).

To calculate BMC in each sub-volume, firstly, the grayscale VOI datasets were smoothed with a Gaussian filter (convolution kernel [3 3 3], standard deviation=0.65) and then binarised into bone and background using a fixed single level threshold, i.e. 25.5% of maximal grayscale value (around 420 mg HA/ccm) (Klinck et al., 2008), close to the values applied in other studies performed on mouse bone with the same image resolution (Birkhold et al., 2014; Lambers et al., 2015; Lukas et al., 2013). The BMC in each sub-volume was calculated as the volume of image voxel times the Bone Mineral Density (BMD) values summed over all bone voxels. In addition, the cortical and trabecular compartments were separated (Bue et al., 2007) and the total BMC for each bone type [Ct.BMC and Tb.BMC] was calculated.

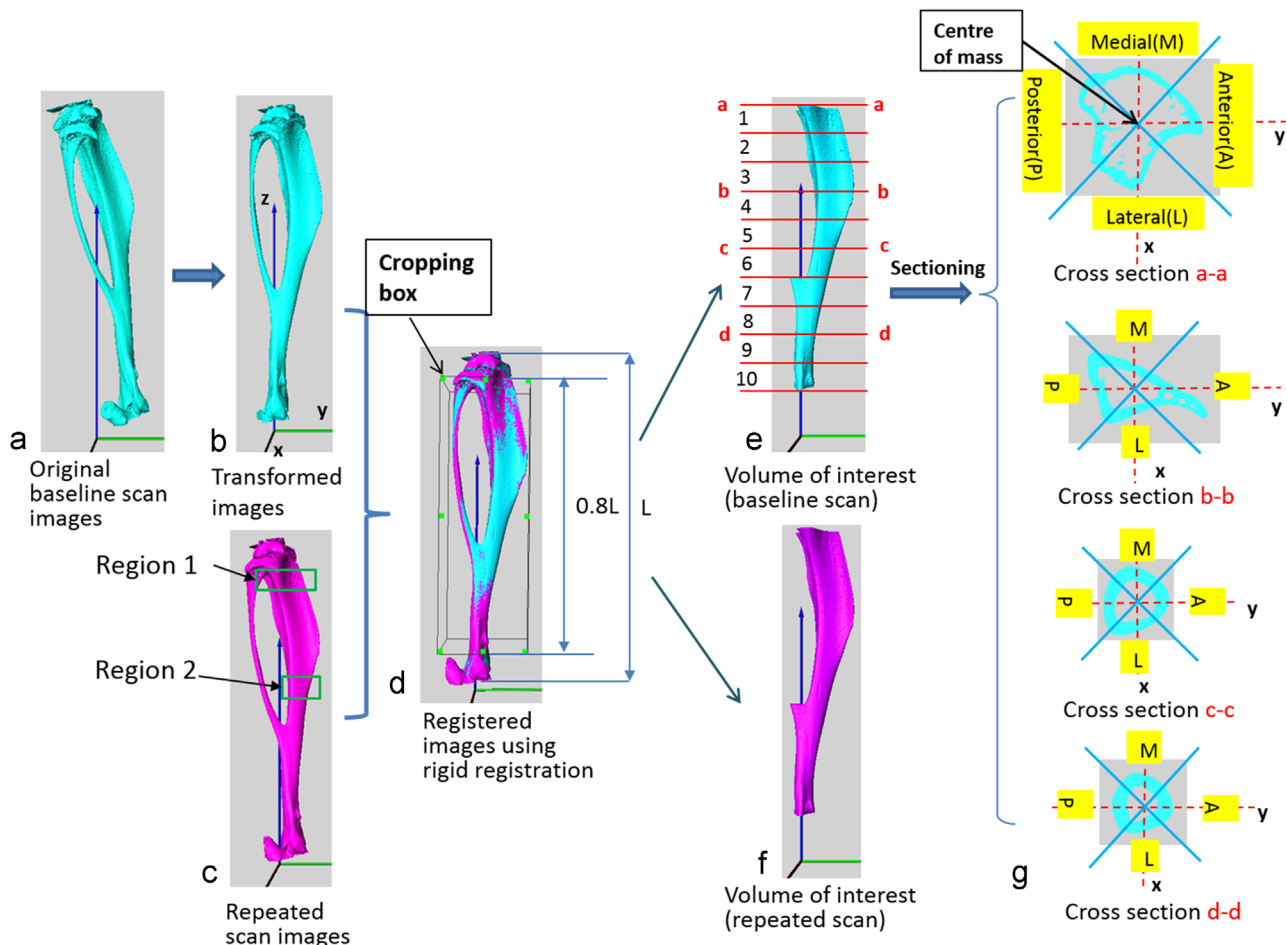


Fig. 1. Overview of the image processing chain in the reproducibility study.

Following the standard procedure, the bone morphometric measurements were quantified in order to ensure the quality of the images by comparing with literature data. Trabecular bone volume fraction (Tb.BV/TV), trabecular thickness (Tb.Th), trabecular separation (Tb.Sp), trabecular number (Tb.N) were computed in the region (Region 1 in Fig. 1c) extending 1.00 mm distally from the growth plate, with an offset of 0.20 mm from the most distal break in the calcified cartilage bridge of the growth plate observed in the grayscale CT slice (Nishiyama et al., 2010; Klinck et al., 2008). Cortex thickness (Ct.th) was calculated in a 1.00 mm region centred at the tibial mid-shaft (Region 2 in Fig. 1c).

2.4. Statistical analysis

The reproducibility of the global and local bone mineral content variables was characterized by the precision errors (PEs) (Glueer et al., 1995), the least significant change (LSCs) (Burghardt et al., 2013; Shepherd and Lu, 2007) and the intraclass correlation coefficients (ICCs) (Shrout and Fleiss, 1979). PEs were expressed as the coefficients of variation (CV) (PE_{%CV}).

$$PE_{\%CV} = \sqrt{\frac{\sum_{j=1}^m \%CV_j^2}{m}} \tag{1}$$

with

$$\%CV_j = \frac{SD_j}{\bar{x} \times 100\%} \tag{2}$$

where, *m* is the subject number (*m*=8 in the current study) and \bar{x}_j is the mean of all x_{ij} for subject *j*.

The LSC was calculated as follows:

$$LSC = Z \times PE_{\%CV} \sqrt{\frac{1}{n_1} + \frac{1}{n_2}} \tag{3}$$

where, *Z*-score corresponds a two-tailed 95% confidence level (*Z*=1.96), while *n*₁ and *n*₂ are the number of measures performed at baseline (*n*₁) and follow-up (*n*₂), respectively.

The ICC is the ratio of the between-subject variance divided by the population variance (Nishiyama et al., 2010).

$$ICC = \frac{F_0 - 1}{F_0 + (n - 1)} \tag{4}$$

where, *F*₀ is the ratio of between-subject mean squares over the residual within-subject mean squares and *n* is the number of repetitions (*n*=4 in this study).

3. Results

The tibial length has a PE_{%CV} of 0.11%, a LSC of 0.13% and an ICC of 0.99. Bone morphometric parameters have PE_{%CV} ranging from 0.49% (Ct.Th) to 3.59% (Tb.BV/TV), LSC from 0.56% to 4.14%, and ICCs from 0.93 (Tb.Sp) to 0.99 (Ct.Th), the values of which are comparable to the data in literature (Fig. 2). The Ct.BMC and Tb.BMC have PE_{%CV} of 1.58% and 3.04%, LSC of 1.82% and 3.51%, and ICCs of 0.95 and 0.98, respectively.

Regarding the local BMC measurements, 24 out of 40 regions (60%) have PE_{%CV} less than 2%, 15 regions (37.5%) between 2% and 3%, and one region (2.5%) with 3.2%

(Fig. 3). LSCs for the 40 regions were less than 3.80%, ranging from 1.46% to 3.78%. 29 out of 40 regions (72.5%) have ICCs over 0.90, 9 regions (22.5%) between 0.80 and 0.90 (Fig. 3). With respect to the anatomical location of the tibia, there is no spatial variability pattern for the reproducibility.

The mean ± SD values of tibial morphometric measurements, global and local BMC measurements, and their precision errors and ICCs are reported in Appendix A, Table A.1.

4. Discussion

In this study, a novel protocol, which can take into account large bone growth, was developed to quantify local bone adaptations over space and time. High precision and reproducibility of the local BMC measurements, calculated through the protocol, were found. Although the reproducibility values cannot be directly migrated to the images obtained from other μCT systems or other voxel size scans with the same system (Verdelis et al., 2011), this paper proposed a protocol to evaluate local bone adaptations over space and time and this protocol is irrespective of the μCT systems and μCT voxel size.

The proposed protocol was made efficient by selecting 80% of the tibial length as the VOI to represent the entire tibia. The tibial growth plates were excluded, which not only cause noise and errors in the calculation of BMC, but also impede the automation of the protocol. The BMC was selected as the parameter to quantify local bone adaptation, but other parameters, e.g. periosteal/endocortical perimeters, bone marrow area, etc. (Bouxsein et al., 2010), can be quantified using the protocol developed in this study.

In this paper, the tibial VOI was partitioned into 40 sub-volumes. Our preliminary investigations showed there was a conflict between the desire to quantify bone adaptation with the highest possible spatial resolution, and the need for highly reproducible measurements. We found that the partitioning proposed is a reasonable compromise between these two conflicting needs and that smaller compartments would provide less reproducible measurements (Table A.2 in the Appendix), and larger compartments would not further reduce it while losing spatial resolution.

When investigating bone adaptations using rodents, there are essentially two scenarios: the first is that bone undergoes significantly low growth during the experiment (e.g. adult rat or caudal vertebra of adult mouse with the scanning interval of one week) (Altman et al., 2015; Birkhold et al., 2014). In such case, the voxel difference between the superposed images transformed with the rigid registration (Birkhold et al., 2014; Lambers et al., 2013; Schulte et al., 2011) or the distance vectors between the bone iso-surfaces (Lu et al., 2015) can be interpreted as bone formation and resorption. The second is that bone undergoes continuous relatively large growth (e.g. mouse tibia) during the experiment (Fig. 4). In such case, the previous methods would produce erroneous results and the bone changes could be measured by using a full elastic registration approach that could be adapted from (Dall’Ara et al., 2014) or the affine scaling of anatomically referenced partitioning, which was applied in the current study. Our preliminary investigation (Table A.2 in the Appendix) showed that when using smaller size of compartments over which the BMC is averaged would considerably degrade the reproducibility of the measurements. This strongly suggested that when dealing with the bone with large growth, the image voxel-level comparisons need to be replaced with the protocol proposed in this study, which can take into account the relatively large bone growth.

In conclusion, a novel protocol, which can take into account large bone growth, was developed to quantify local bone adaptation over space and time and high reproducibility of the local BMC measurements was found. In the future, the protocol can be used

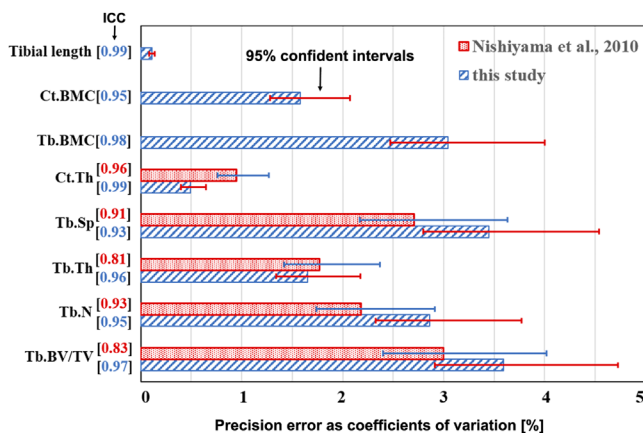


Fig. 2. Reproducibility of mouse cortical and trabecular parameters (tibial length, tibial cortex BMC, trabecular BMC and tibial morphometric parameters) expressed in precision error as coefficients of variation (PE_{%CV}) and the 95% confident intervals (CI_{95%}) shown in terms of error bars, and the intraclass correlation coefficients (ICC) are reported in square brackets (8 mice and 4 scans per mouse).

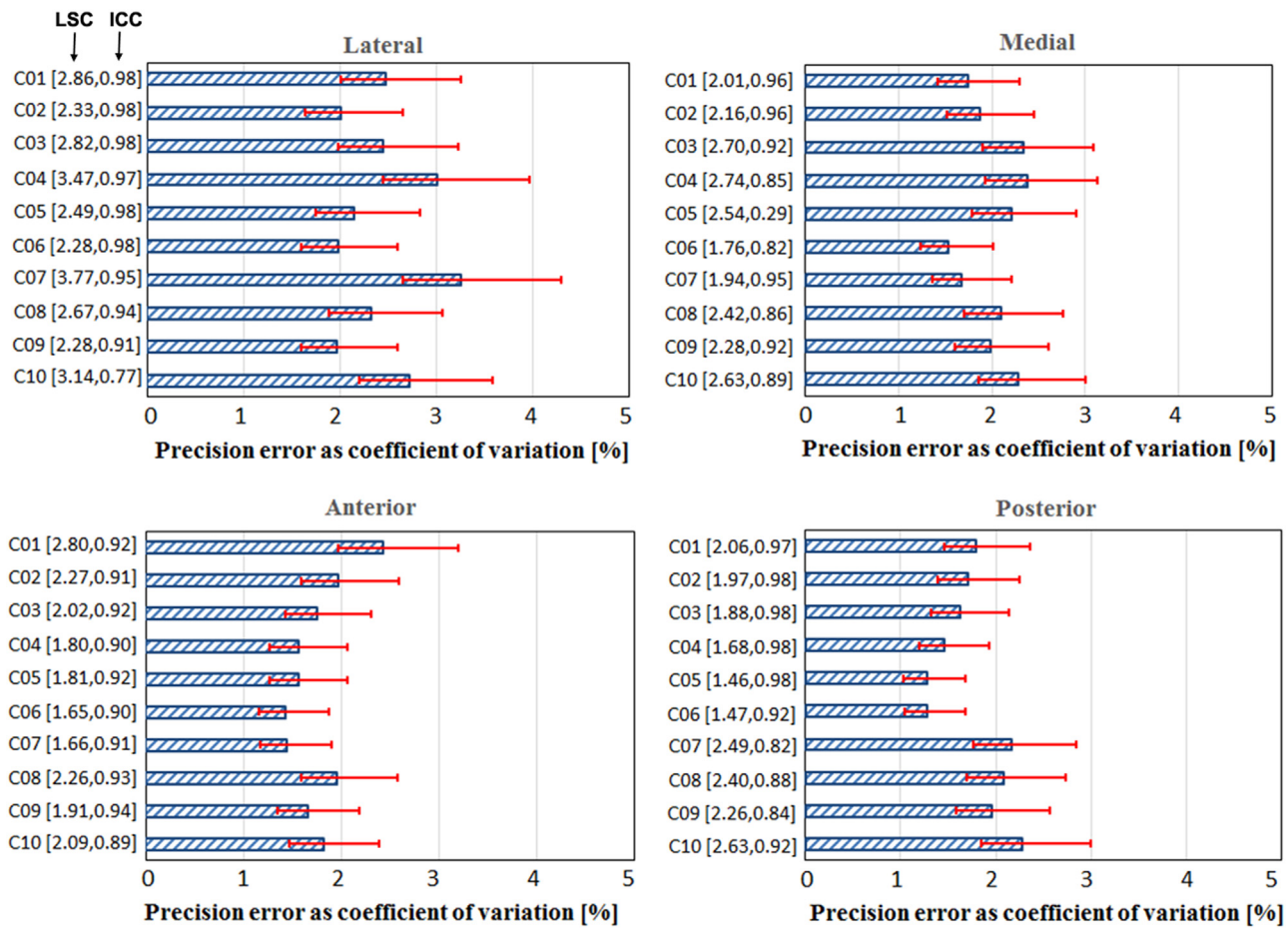


Fig. 3. Reproducibility of the mouse tibial local BMC expressed in mean precision error as coefficients of variation ($PE_{\%CV}$) and the 95% confident intervals ($CI_{95\%}$) shown in terms of error bars, the least significant change (LSC) and the intraclass correlation coefficients (ICC) are reported in square brackets (8 mice and 4 scans per mouse) (C01–C10 corresponds tibial proximal to distal side, see Fig. 1e).

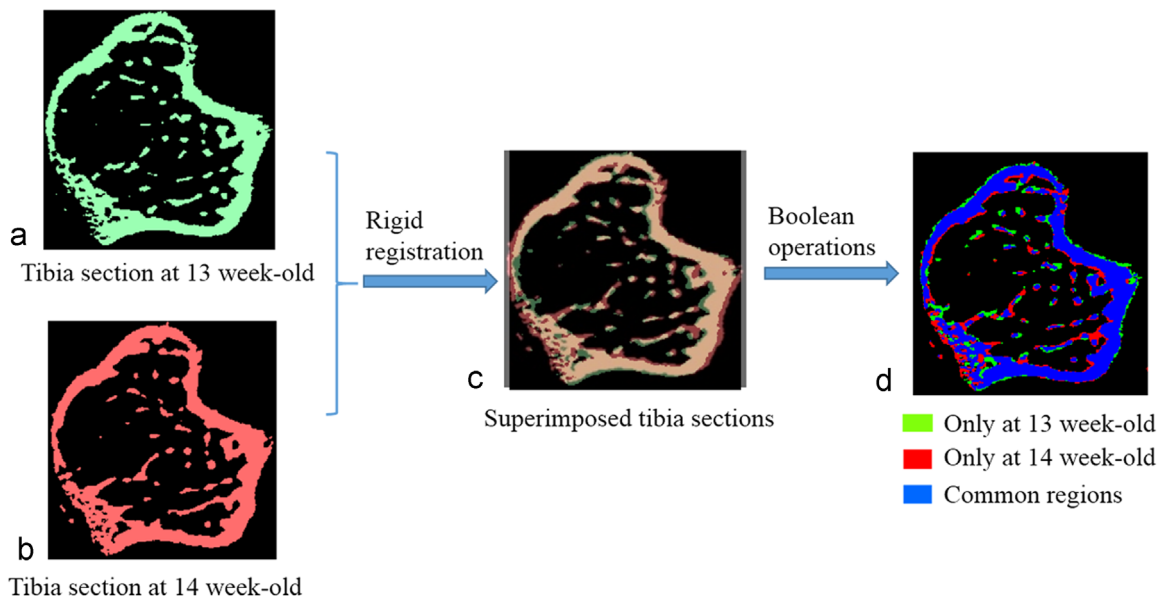


Fig. 4. Superimposition of two mouse tibia sections (a and b) using the rigid registration and visualisation of bone adaptations (d). Over one week, there is little common regions in the trabecular part due to the relatively large growth.

in longitudinal image datasets to quantify local bone adaptation over space and time.

Conflict of interest statement

The authors have no conflicts to declare.

Acknowledgements

This work was funded by the UK National Centre for the Replacement, Refinement and Reduction of Animals in Research (NC3Rs), grant number:NC/K000780/1, the Engineering and Physical Sciences Research Council – MultiSim project, grant number: EP/K03877X/1 and the Chinese Fundamental Research Funds for the Central Universities, project number: DUT15RC(3)130.

Appendix A. Supplementary material

Supplementary data associated with this article can be found in the online version at <http://dx.doi.org/10.1016/j.jbiomech.2016.05.022>.

References

- Altman, A.R., Tseng, W.J., de Bakker, C.M.J., Chandra, A., Lan, S., Huh, B.K., Luo, S., Leonard, M.B., Qin, L., Liu, X.S., 2015. Quantification of skeletal growth, modelling, and remodelling by in vivo micro computed tomography. *Bone* 81, 370–379.
- Birkhold, A.I., Razi, H., Duda, G.N., Weinkamer, R., Checa, S., Willie, B.M., 2014. The influence of age on adaptive bone formation and bone resorption. *Biomaterials* 35, 9290–9301.
- Bouxsein, M.L., Boyd, S.K., Christiansen, B.A., Guldberg, R.E., Jepsen, K.J., Mueller, R., 2010. Guidelines for assessment of bone microstructure in rodents using micro-computed tomography. *J. Bone Miner. Res.* 26 (7), 1468–1486.
- Britton, C., Walsh, J., 2012. Paget disease of bone – an update. *Aust. Fam. Physician* 41 (3), 100–103.
- Buie, H.R., Campbell, G.M., Klinck, R.J., MacNeil, J.A., Boyd, S.K., 2007. Automatic segmentation of cortical and trabecular compartments based on a dual threshold technique for in vivo micro-CT bone analysis. *Bone* 41 (4), 505–515.
- Burghardt, A.J., Pialat, J.-B., Kazakia, G.J., Boutroy, S., Engelke, K., et al., 2013. Multi-center precision of cortical and trabecular bone quality measures assessed by HR-pQCT. *J. Bone Miner. Res.* 28 (3), 524–536.
- Campbell, G.M., Tiwari, S., Grundmann, F., Purcz, N., Schen, C., Glueer, C.-C., 2014. Three-dimensional image registration improves the long-term precision of in vivo micro-computed tomographic measurements in anabolic and catabolic mouse models. *Calcif. Tissue Int.* 94, 282–292.
- Dall'Ara, Barber D., Viceconti, M., 2014. About the inevitable compromise between spatial resolution and accuracy of strain measurement for bone tissue: a 3D zero-strain study. *J. Biomech.* 47 (12), 2956–2963.
- Glatt, V., Canalis, E., Stadmeier, L., Bouxsein, M.L., 2007. Age-related changes in trabecular architecture differ in female and male C57BL/6J mice. *J. Bone Miner. Res.* 22 (8), 1197–1207.
- Glueer, C., Blake, G., Lu, Y., Blunt, B.A., Jergas, M., Genant, H.K., 1995. Accurate assessment of precision errors: how to measure the reproducibility of bone densitometry techniques. *Osteoporos. Int.* 5 (4), 262–270.
- Klinck, R.J., Campbell, G.M., Boyd, S.K., 2008. Radiation effects on bone architecture in mice and rats resulting from in vivo micro-computed tomography scanning. *Med. Eng. Phys.* 30, 888–895.
- Lambers, F.M., Koch, K., Kuhn, G., Ruffoni, D., Weigt, C., Schulte, F.A., Mueller, R., 2013. Trabecular bone adapts to long-term cyclic loading by increasing stiffness and normalisation of dynamic morphometric rates. *Bone* 55 (2), 325–334.
- Lambers, F.M., Kuhn, G., Weigt, C., Koch, K.M., Schulte, F.A., Mueller, R., 2015. Bone adaptation to cyclic loading in murine caudal vertebrae is maintained with age and directly correlated to the local micromechanical environment. *J. Biomech.* 48 (6), 1179–1187.
- Laperre, K., Depypere, M., van Gestel, N., Torrekens, S., Moermans, K., Bogaerts, R., et al., 2011. Development of micro-CT protocols for in vivo follow-up of mouse bone architecture without major radiation side effects. *Bone* 49 (4), 613–622.
- Lu, Y., Boudiffa, M., Dall'Ara, E., Bellantuono, I., Viceconti, M., 2015. Evaluation of in vivo measurements errors associated with micro-computed tomography scans by means of the bone surface distance approach. *Med. Eng. Phys.* 37 (11), 1091–1097.
- Lukas, C., Ruffoni, D., Lambers, F.M., Schulte, F.A., Kuhn, G., Kollmannsberger, P., Weinkamer, R., Mueller, R., 2013. Mineralization kinetics in murine trabecular bone quantified by time-lapsed in vivo micro-computed tomography. *Bone* 56 (1), 55–60.
- Nishiyama, K.K., Campbell, G.M., Klinck, R.J., Boyd, S.K., 2010. Reproducibility of bone micro-architecture measurements in rodents by in vivo micro-computed tomography is maximized with three-dimensional image registration. *Bone* 46 (1), 155–161.
- Schulte, F.A., Lambers, F.M., Kuhn, G., Mueller, R., 2011. In vivo micro-computed tomography allows direct three-dimensional quantification of bone formation and bone resorption parameters using time-lapsed imaging. *Bone* 48 (3), 433–442.
- Shepherd, J.A., Lu, Y., 2007. A generalized least significant change for individuals measured on different DXA systems. *J. Clin. Densitom.* 10 (3), 249–258.
- Shih, M.S., 2012. Bone adaptation in osteoporosis. *Curr. Osteoporos. Rep.* 10 (3), 187–189.
- Shrout, P., Fleiss, J., 1979. Intraclass correlations: uses in assessing rater reliability. *Psychol. Bull.* 86 (2), 420–428.
- Turkowski, K., Gabriel, S., 1990. Filters for common resampling tasks. In: Glassner, A.S. (Ed.), *Graphics Gems 1*. Academic Press, pp. 147–165.
- Verdelis, K., Lukashova, L., Atti, E., Mayer-Kuckuk, P., Peterson, M.G.E., Tetradis, S., Boskey, A.L., van der Meulen, M.C.H., 2011. MicroCT morphometry analysis of mouse cancellous bone: intra- and inter-system reproducibility. *Bone* 49 (3), 580–587.